

Roadmap on machine learning glassy dynamics

Gerhard Jung^{1,2}, Rinske M. Alkemade³, Victor Bapst⁴, Daniele Coslovich⁵, Laura Filion³, François P. Landes⁶, Andrea J. Liu^{7,8}, Francesco Saverio Pezzicoli⁶, Hayato Shiba⁹, Giovanni Volpe¹⁰, Francesco Zamponi¹¹, Ludovic Berthier^{1,12}✉ & Giulio Biroli¹³

Abstract

Unravelling the connections between microscopic structure, emergent physical properties and slow dynamics has long been a challenge when studying the glass transition. The absence of clear visible structural order in amorphous configurations complicates the identification of the key physical mechanisms underpinning slow dynamics. The difficulty in sampling equilibrated configurations at low temperatures hampers thorough numerical and theoretical investigations. We explore the potential of machine learning (ML) techniques to face these challenges, building on the algorithms that have revolutionized computer vision and image recognition. We present both successful ML applications and open problems for the future, such as transferability and interpretability of ML approaches. To foster a collaborative community effort, we also highlight the ‘GlassBench’ dataset, which provides simulation data and benchmarks for both 2D and 3D glass formers. We compare the performance of emerging ML methodologies, in line with benchmarking practices in image and text recognition. Our goal is to provide guidelines for the development of ML techniques in systems displaying slow dynamics and inspire new directions to improve our theoretical understanding of glassy liquids.

Sections

Introduction

Machine learning locally favoured structures

Prediction of structural relaxation and dynamic heterogeneities

Learning phenomenological glass models

Performance metrics and benchmarking

Outlook

¹Laboratoire Charles Coulomb (L2C), Université de Montpellier, CNRS, Montpellier, France. ²Laboratoire Interdisciplinaire de Physique (LIPhy), Université Grenoble Alpes, Saint-Martin-d’Hères, France. ³Soft Condensed Matter and Biophysics, Debye Institute for Nanomaterials Science, Utrecht University, Utrecht, The Netherlands. ⁴GoogleDeepMind, London, UK. ⁵Dipartimento di Fisica, Università di Trieste, Trieste, Italy. ⁶TAU Team, Laboratoire Interdisciplinaire des Sciences du Numérique, CNRS, INRIA, Université Paris-Saclay, Gif-sur-Yvette, France. ⁷Department of Physics and Astronomy, University of Pennsylvania, Philadelphia, PA, USA. ⁸Santa Fe Institute, Santa Fe, NM, USA. ⁹Graduate School of Information Science, University of Hyogo, Kobe, Japan. ¹⁰Department of Physics, University of Gothenburg, Gothenburg, Sweden. ¹¹Dipartimento di Fisica, Sapienza Università di Roma, Rome, Italy. ¹²Gulliver, UMR CNRS 7083, ESPCI Paris-PSL Research University, Paris, France. ¹³Laboratoire de Physique de l’Ecole Normale Supérieure, ENS Université PSL, CNRS, Sorbonne Université, Université de Paris, Paris, France. ✉e-mail: ludovic.berthier@espci.fr

Key points

- Systematic characterization of amorphous glassy structures can be addressed by unsupervised learning, which requires an adequate choice of structural descriptors.
- Finding structure–dynamics relationships in glassy liquids is a task that has many analogies with image recognition and can be tackled using supervised learning with various neural network architectures already successful in image recognition.
- Major challenges and potential breakthroughs await in transferring trained models to extremely low temperatures, using them to create ultrastable glasses and design new phenomenological glass models.
- Future directions also encompass generative modelling of low-temperature equilibrium configurations and development of self-supervised and reinforcement learning approaches.
- Publicly available datasets and unified benchmarks that are fundamental to stimulate further development of ML techniques in condensed matter physics are provided.

Introduction

When supercooled liquids undergo a glass transition, a dramatic slowdown of transport properties is observed and the resulting material dynamically resembles a crystalline solid, yet one of the main characteristic of glasses is that they maintain their amorphous liquid structure¹. Despite several decades of research involving experiments, theory and computer simulations, many fundamental mechanisms remain to be elucidated, such as macroscopic mechanical properties, highly cooperative stress relaxation in glasses, and the statistical mechanics nature of the glass transition itself².

The rise of deep learning in the past decade³ was initially driven by applications in computer vision, in particular image recognition and feature detection, fields in which deep learning soon outperformed traditional techniques⁴. These original breakthroughs are now starting to revolutionize several other areas in technology and science. Our aim in this Technical Review is to address the potential of ML methods to boost research on fundamental aspects of glassy dynamics, in particular the ones that have an important role in advancing theories of the glass transition.

In this Technical Review, we identify three challenges in developing a fundamental microscopic theory of glasses. One challenge is the absence of any simple and visible structural order. Crystalline defects in otherwise well-ordered structures are easily detectable, but finding analogous structural features in amorphous materials remains an open problem. Over the years, many different proposals for ‘defects’ or locally favoured structures have been proposed and developed^{5–8}. This variety of proposals seems to indicate that even in amorphous configurations, it could be possible to detect the emergence of some kind of short-range and medium-range order. However, these identifications usually only apply to specific systems, and they are often only weakly correlated with local dynamical relaxations. There is, therefore, a clear need for new and more powerful system-independent ways to systematically find preferred structures in amorphous configurations. This is a challenge for which new ML methods could be a great asset,

in particular owing to the progress in unsupervised learning. Several approaches are being developed towards this goal^{9–12}.

Another long-standing challenge has been understanding and characterizing the fundamental mechanisms underpinning slow and glassy dynamics, which are responsible for the glass transition. To this aim, there has been a substantial effort to identify the microscopic properties that lead to dynamical relaxation. Given a snapshot (an equilibrium configuration), several local properties have been proposed to pinpoint the regions that have higher tendency to relax within a window of, say, some fraction of the relaxation time. Examples include the local Debye–Waller factor, eigenvectors of the Hessian of inherent structures, and so on^{13,14}. There is no consensus on what is the best predictor of future dynamics. Moreover, the best choice could change with temperature or be system-specific, according to several theories of the glass transition¹⁵. Owing to the advances in numerical simulations of glass-forming liquids, it is now possible to produce large datasets of initial configurations and subsequent dynamical trajectories. This provides a natural playground to apply supervised learning techniques in order to identify the local predictors of dynamical relaxation. Several researchers have taken up this challenge and developed ML methods to predict where local relaxations have higher tendency to take place given an initial snapshot^{16–27}.

Finally, the ultimate goal of the research efforts devoted to the theory of glassy dynamics would be to combine the solutions of the previous problems to develop an effective theory of the glass transition. Until now, this challenge has been tackled starting from some theoretical assumptions driven by experimental and simulation results¹⁵. ML methods can also make a difference in this challenge; they can assist in this quest by providing a complementary identification of the mechanisms inducing relaxation²⁸.

The time is ripe to investigate the ability of ML methods to advance the fundamental understanding of glass-forming liquids. In this Technical Review, focusing on the three main goals described above, we present the recent contributions in this endeavour, discussing the main difficulties ahead and possible paths to circumvent them. In Fig. 1, we give a visual overview over the different ML concepts that will be discussed within the individual sections. We then describe a framework ‘GlassBench’²⁹ intended to enable, encourage and structure a broader community effort to further develop such ML approaches. GlassBench consists of a dataset including simulation data for a 2D²⁷ and a 3D glass former^{22,30}, benchmarks on different tasks associated to predicting local dynamics from a given initial configuration, and an assessment of the state of the art. Our purpose is to fuel and organize new developments of advanced ML techniques, as done in the field of image and text recognition, as well as generative modelling. (See, for example, [benchmarks](#) in the fields of computer vision, natural language processing, time series analysis and much more.) Finally, we discuss future directions for research.

Machine learning locally favoured structures

Although glass-forming liquids and glasses lack long-range order, close inspection of their atomic structure reveals particle arrangements that are more regular, symmetric and of lower (free) energy than the average. Icosahedral local structures are the best known example of such favourable arrangements, and they are found in several metallic alloys, colloidal suspensions and computer models of glassy liquids⁵. Such locally favoured structures (LFSs), distinct from the bulk of the particle arrangements and yet incompatible with crystalline order, are also key ingredients of some theoretical approaches to glass formation^{15,31}.

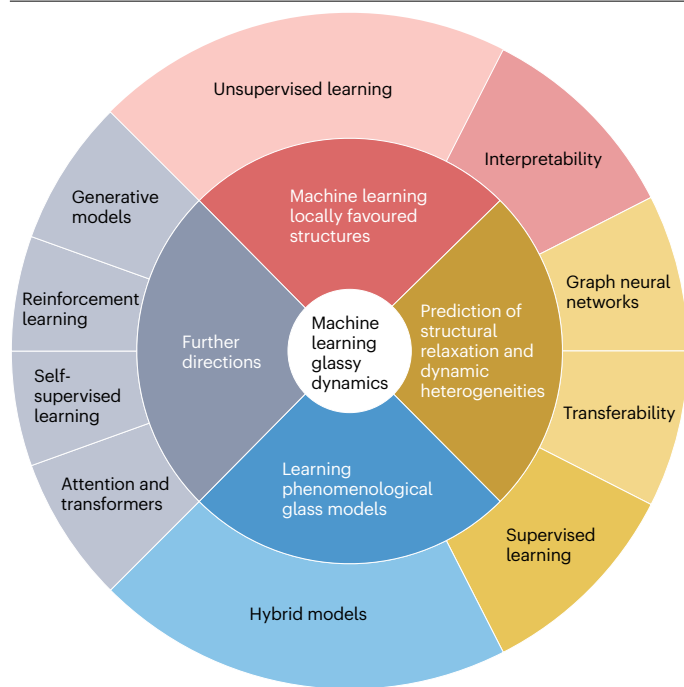


Fig. 1 | Visual summary of the scope of this Technical Review. The individual sections at the centre are connected to the big questions in the field of glass physics. They are surrounded by the various machine learning concepts used to answer them.

Despite the importance of structural analysis in glassy materials^{5,6}, there is at present no generally accepted operational definition of LFS. Standard approaches – such as Voronoi tessellation³², topological cluster classification³³ and other related methods^{34,35} – provide a detailed classification of the possible local geometric arrangements. These methods may indicate which local arrangements are the most abundant or most stable, but they are sensitive to thermal fluctuations and tend to provide a too fine-grained classification, which is difficult to exploit in a theoretical setting. Bond-order parameters (BOPs)³⁶ provide yet another way to characterize the local structure of dense particle systems⁶. Although this approach offers in principle a systematic description of the local arrangements, the choice of the relevant BOP has traditionally been guided by physical intuition⁶, which requires specific and system-dependent a priori knowledge about the relevant symmetries of the local arrangements.

Unsupervised learning methods offer natural system-independent ways to tackle the above issues^{37–40}. Along with automated identification of phase transitions^{41–43}, one of the key applications of unsupervised learning in condensed matter physics is characterization of the properties of complex materials from high-dimensional datasets³⁸. The general idea is to first characterize a faithful, high-dimensional representation of the particle local environment based, for instance, on a systematic bond-order expansion of the local density⁴⁴ (see ref. 45 for a review on structural descriptors). Unsupervised ML methods are then used to identify a small number of collective coordinates, \bar{X}_i , that account for the relevant fluctuations of the local structure, thereby reducing the dimensionality of the descriptors.

Dimensionality reduction techniques range from simple principal component analysis (PCA), or its kernel variant, to more sophisticated statistical learning methods, such as neural network auto-encoders (AEs)³⁷. These methods may in future be combined with more advanced approaches, such as self-supervised learning or pre-training (as discussed in the section ‘Self-supervised, semi-supervised and reinforcement learning’), possibly exploiting the intrinsic symmetries of the system⁴⁶. Once the reduced structural representation of the material structure is obtained, clustering methods can be applied to pinpoint its heterogeneity³⁸.

The studies highlighted in ref. 38 focus mostly on ordered materials or disordered systems with covalent or hydrogen bonding, such as amorphous carbon⁴⁷ or liquid water⁴⁸, in which the preferred geometrical order is readily identified owing to low coordination numbers. Dense amorphous systems are characterized instead by close-packed arrangements, which provide a challenging benchmark for this kind of structural analysis. In a series of papers^{9,10,49–51}, dimensionality reduction and clustering were applied to models of closed-packed glass-forming liquids. In particular, BOPs, Gaussian mixture models and a neural network AE have been used to reveal⁹ a significant structural heterogeneity in glassy binary mixtures, suggesting that in these systems, one can distinguish fluctuating regions that display two different types of local disorder. The spatial heterogeneity of these regions is also correlated with the dynamic structural relaxation in the system. Such structure–dynamics correlations are further discussed in the next section.

A related study in ref. 10 has addressed the issue of clustering of local structural arrangements using a different, information-theoretic approach. At a qualitative level, the results of the analysis in refs. 9 and 10 appear consistent with one another. However, a more recent investigation⁴⁹ revealed a notable system-dependence of structural heterogeneity in glassy liquids. The gist of these findings is illustrated in Fig. 2, which shows representative PCA maps obtained from a smooth bond-order (SBO) descriptor (more details are given in the Supplementary information). The distribution of the first two principal components is bimodal for an embedded-atom model of Cu₆₄Zr₃₆, which has a well-defined icosahedral LFS, whereas it is less heterogeneous for the canonical Kob–Andersen (KA) mixture (which will be benchmarked in the section ‘Performance metrics and benchmarking’), whose local arrangements display a homogeneous distribution of geometrical states. Although these differences question the universality of the concept of LFS, the first few principal component projections always correlate with physically motivated structural measures⁴⁹.

We expect that more information could be harvested by looking at chemically resolved descriptors⁵² and on larger length scales (medium-range order). Moreover, computing the intrinsic dimension of structural datasets^{43,53} may provide additional insight into the nature of structural order and its system dependence.

A striking observation reported in ref. 49 is that neural network AE and PCA yield identical reductions of the BOP descriptors. This finding suggests at least two possible scenarios. The first possibility is that the local structure in dense glassy mixtures is simple: it displays a broad continuous spectrum of geometrical arrangements, possibly decorated by features such as LFS, crystallites or structural defects. The second possibility is that the current identification of LFS is missing some crucial ingredient. The outcome of PCA is also straightforward to interpret because the principal component directions provide direct insight into the dominant structural parameters. In the presence of agnostic, high-dimensional structural descriptors, such as the smooth

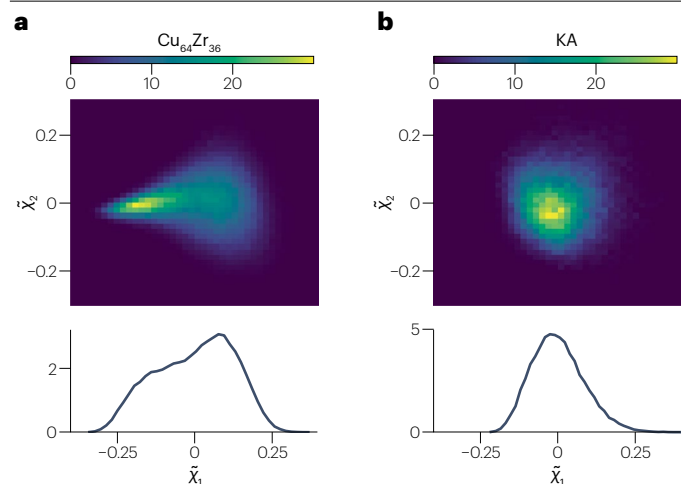


Fig. 2 | Principal component analysis maps of the first two principal component projections \tilde{X}_1 and \tilde{X}_2 of the smooth bond-order (SBO) parameter in two representative systems. a, SBO parameter around Cu atoms in glassy $\text{Cu}_{64}\text{Zr}_{36}$. **b**, SBO parameter around small particles in the Kob-Andersen (KA) binary mixture around its mode-coupling temperature⁴⁹. Note the contrast between the bimodal structure in part **a** owing to icosahedral local structures⁴⁹ and the homogeneous distribution of the projections in part **b**. The bottom panels show the marginal distribution of the first principal component projection.

atomic overlap parameters⁴⁴, interpretation always occurs a posteriori, by searching for correlations between some of the reduced structural and physically motivated structural measures³⁸.

On the one hand, these results question the utility of complex deep learning methods in studying glass structure. On the other hand, the descriptors used in refs. 9,10,49 do not exhaust all forms of structural heterogeneity, and some may be affected by some deeper shortcomings⁵⁴. Development of structural descriptors remains active^{55,56}, and these advances wait for applications in the context of glassy materials. Addressing the above issues may become crucial in future studies of more demanding benchmarks for structural characterization, such as compositional order in polydisperse glassy models^{57,58}, medium-range order in oxides or metallic glasses^{59,60}, and orientational order in glassy water^{61,62}. Computational studies of these complex systems represent opportunities to gain insight into the nature and role of local structure in glassy materials and to provide solid grounds for predictive theoretical approaches based on structure.

Another research line wherein structure-based ML approaches are making progress aims at predicting macroscopic properties of glasses relevant for applications, such as oxides or chalcogenide glasses, over a wide range of chemical compositions^{63,64}. Work on sodium-silicate glasses shows that physics-informed machine learning models can reliably interpolate and extrapolate these properties based on structural information only⁶⁵. These findings indicate that, despite the apparent complexity of the feature space, the relationship between local structure and macroscopic glass properties is often linear, which makes it simple for machine learning models to generalize outside their training set (see ref. 66 for a roadmap on this topic).

Having characterized amorphous structure, a crucial question is whether the structural descriptors are connected to emergent relaxation dynamics in the glass-forming liquid^{13,67–69}. As will be clear in the section ‘Performance metrics and benchmarking’, present-day

unsupervised methods provide only limited insights into the heterogeneity of the dynamics, except in specific systems dominated by strong icosahedral order^{9,10,49}. Whether this is a technical limitation of the unsupervised methods used to date, or is an intrinsic feature of supercooled dynamics, remains to be clarified.

Prediction of structural relaxation and dynamic heterogeneities

One of the central challenges for both computational and theoretical studies of glass-forming liquids is to use an initial snapshot to predict the future dynamics of a configuration. Note that one is not interested in predicting the whole future evolution but only the dynamical processes leading to microscopic irreversible motion. Supervised ML provides a natural tool to perform such prediction, essentially by fitting high-dimensional structural input to the relaxation dynamics, similar in spirit to classification in image recognition. In general, three choices need to be made to design a model: which structural descriptors to use to characterize the input configuration, which labels to use to quantify structural microscopic relaxation, and what model and ML algorithm to use to fit the input to the labels. Varied techniques have already been introduced to tackle this problem, ranging from ridge regression using complex and coarse-grained structural descriptors to graph neural networks using raw particle positions (Fig. 3).

Support vector classifiers (SVCs) have been used to classify soft spots relaxing fast against slowly relaxing regions in glasses¹⁷. (Note that in ref. 17, the term support vector machine was used, but here we use the term support vector classifier to stress the fact that the procedure corresponds to a classification and not a regression.) Here, soft spots are defined as regions that have a high likelihood of rearranging within a short timescale. As input to this algorithm, each particle is assigned a vector of local structural descriptors that captures the local density and angular structure within shells at different distances from its centre. From the trained SVC, a quantity called softness, S , can be extracted, which correlates with the likelihood for the particle to rearrange in the near future. Softness has been used to gain insight into a variety of glass problems that encompass many types of glassy liquids and disordered solids, ranging from strong to fragile and ductile to brittle, with constituent particles ranging from atomic to granular, studied in bulk and in thin films^{16,70–78}. Furthermore, this approach also led to a series of papers^{28,79,80} aiming at constructing an effective model for the dynamics in glassy fluids built around the evolution of the softness field, which will be discussed in more detail in the next section.

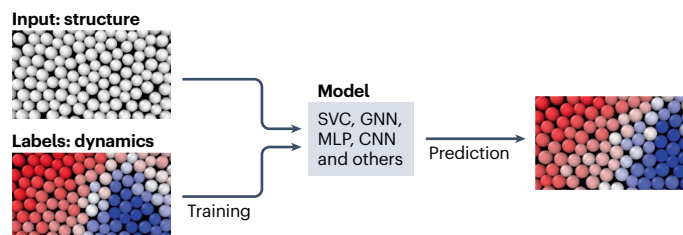


Fig. 3 | Typical supervised machine learning (ML) procedure in condensed matter. The raw input is encoded using structural descriptors or graphs. A model is trained using labels that describe structural relaxation obtained from, for example, molecular dynamics simulations. Colours indicate frozen (blue) or rearranging (red) particles. ML techniques include support vector classification (SVC), graph neural networks (GNNs), multilayer perceptrons (MLPs) and convolutional neural networks (CNNs). After training, structural relaxation is predicted for previously unseen structures.

Whereas softness is associated to prediction on short timescales, several subsequent works have focused on predicting the dynamics, or more precisely the dynamic propensity⁸¹, on longer timescales $t \approx \tau_\alpha$. Here, τ_α is the typical structural relaxation timescale on which each particle moves on average approximately one particle diameter (see the Supplementary information for more details). Dynamic propensity quantifies the local dynamics of a glass-forming liquid by capturing the typical behaviour of each particle in a structure using the isoconfigurational ensemble⁸¹. This ensemble is formed by a set of trajectories that start from the same initial structure but with different initial velocities drawn from a Maxwell–Boltzmann distribution. By calculating the mean distance travelled by a given particle in this ensemble, one arrives at the dynamic propensity $\langle |\Delta \mathbf{r}_i(t)| \rangle_{\text{iso}}$. Owing to this averaging, the dynamic propensity captures the part of the dynamics encoded in the initial structure, leaving out the part stemming from the initial velocities, which cannot be captured by any structural descriptor. Although some dynamical information is necessarily lost⁸², the dynamic propensity, which fluctuates from one particle to the other, is an important measure for dynamic heterogeneity (DH) in supercooled liquids. At the end of this section, we also discuss ways to reintroduce the fluctuations around the isoconfigurational average using different labels or new ML designs.

A graph neural network (GNN) was introduced¹⁸ in 2020 that can predict the dynamic propensity markedly better than a support vector machine (SVM) (wherein the input for the SVM was angular and radial functions similar to ref. 17). In contrast to the SVM, the input to the GNN is a graph structure in which each particle in the initial configuration is represented by a vertex, and edges are drawn between particles within a cut-off radius of each other. In addition to the structure of this graph, the vertices and edges also carry information: the particle species (as vertex data) and the vectors connecting neighbours (as edge data). The GNN model then consists of several multilayer perceptrons (MLPs) that iteratively update the features contained at the edges and nodes, with each iteration passing information along the nodes and edges of the network. After the final iteration, the features at the nodes are passed through a final MLP that predicts the dynamic propensity. As all vertices are updated in parallel, the network predicts mobilities of all particles simultaneously. This network is then optimized to minimize the squared difference between the predicted and true propensity using the \mathcal{L}_2 norm.

Two improvements to this GNN approach have been proposed. A substantially higher accuracy can be reached over nearly all timescales by considering not only single-particle dynamics but also pairwise dynamics²². Specifically, the GNN is trained to predict not only the dynamic propensity but also the isoconfigurational change in the distance between pairs of particles sharing an edge in the graph – a modification called BOnd TArgeting Network (BOTAN)²². Intriguingly, even with the same overall architecture, BOTAN finds a better prediction for the single-particle dynamics, showing that the extra edge information improves the performance of the GNN. An alternative improvement on the GNN approach explicitly requires the GNN to enforce the rotational symmetry, an idea sometimes referred to as geometric deep learning or rotation equivariant network (SE(3)) (ref. 25). This adaptation also improved on the original work in ref. 18 over nearly all considered timescales.

In addition to the development of increasingly sophisticated ML methods to predict the dynamic propensity, efforts have been made to better capture important local features of the structural input. The recursive updating properties of GNNs have been incorporated into a set

of locally coarse-grained structural descriptors²⁰. Fitting just three generations of descriptors with a linear regression algorithm is sufficient to essentially reach the accuracy of the GNN – leading to a far simpler and more interpretable algorithm for fitting glassy dynamics. Interestingly, learning the dynamic propensity using these descriptors with non-linear models (MLP and GNN) does not improve the ability to predict the dynamics, as quantified by the Pearson correlation coefficient²¹.

This approach has been further developed by including physics-inspired descriptors that, in the past 30 years of glass research, have been identified as important structural proxies, in a model known as GlassMLP²⁷. These additional structural descriptors include potential energy and properties of the Voronoi cells, and the choice of describing the system in terms of its inherent state²⁷. The inherent state corresponds to the energy minimum configuration that is closest to the actual input structure. These modifications improve the performance of the network. GlassMLP further uses MLP for supervised learning, which enables the precise representation of non-linear or non-Gaussian features such as probability distributions of propensities²⁷. Using transferability in system size, the network has been applied to determine dynamic correlation lengths and the geometry of rearranging clusters over a wide range of temperatures. The GlassMLP model has been enhanced to improve the transferability across timescales and temperatures and to explore physical regimes wherein direct training cannot be performed⁸³. In a vein similar to GlassMLP, structural descriptors have been improved by going beyond inherent states and by using cage states, in a model known as CAGE²³. In CAGE, cage states are extracted from restricted ensemble averages of the local structure using Monte Carlo simulations. The local environment is, thus, better described, which also helps improve the performance of the model.

By construction, all methods perform best at the temperature at which they are trained. However, it is possible to apply a trained network to other temperatures and test how predictions correlate with true dynamics^{17,18,25,77,83}. Good performance in such transfer experiments indicates that the model captures relevant universal features in the structure–dynamics relationship of glass-forming liquids. Transferability has, for example, been used to investigate links between amorphous structure and fragility⁷⁷ and to predict features of DH for temperatures comparable to the experimental glass transition temperature⁸³. In the section ‘Training a transferable model across different temperatures’, we show additional transferability experiments for several models.

In future work, it will be interesting to further exploit the transferability of supervised ML techniques to robustly extract information on structural relaxation at very low temperatures. One goal would concern the evolution of DH upon approaching the glass transition and make the connection with experimental results⁸⁴. One possible strategy to improve transferability of trained models to low-temperature regimes in which dynamics cannot be run for long enough (that is, regimes in which little or no labelled data is available) would be to use self-supervised learning⁸⁵. More generally, self-supervised learning could also be used to enhance performance of the deep approaches (as discussed in the section ‘Self-supervised, semi-supervised and reinforcement learning’).

To better capture the physical phenomena underpinning glassy dynamics, it is necessary that the ML models not only faithfully predict the dynamics at the single-particle level but also correctly reproduce all statistical features of the propensity field, including spatial and temporal correlations, such as those measured by the four-point susceptibility $\chi_4(t)$ (ref. 86). For GNNs, a known problem is over-smoothing: the predicted propensity field tends to be smoother than the ground

truth. Additional terms can be added to the loss function to prevent over-smoothing, resulting in predictions that display more realistic correlation functions, even in a rather simple MLP architecture²⁷. An open direction is the development of such improved loss functions, which could also be used in deep architectures.

A related idea is to learn not only the isoconfigurational average of the displacement, $\langle |\Delta \mathbf{r}_i(t)| \rangle_{\text{iso}}$, but its full statistical distribution, $P_{\text{iso}}(\Delta \mathbf{r}_i(t))$. This could be accomplished either by additionally fitting higher moments of the distribution or by taking a generative model approach, in which one would generate realistic single-instance dynamical fields (not averaged in the isoconfigurational ensemble). This task could be achieved using a variational auto-encoder approach⁸⁷. Because the spatial correlations of the isoconfigurational average are a priori different from the spatial correlations of single instances, the hope is that such generative models would reproduce these statistics more faithfully than conventional ones. To train such models, information beyond the isoconfigurational average is required, for instance, by providing single-instance configurations, which can also be used to regress the average. Finally, this approach might be able to propose new configurations on the structural relaxation timescale τ_{α} , with the long-term goal being the ability to develop a Monte Carlo algorithm that completely avoids the critical slowing down of the dynamics on the approach to the glass transition. Similarly, the predictions could be used to create ultra-stable glasses by generating prototypical hard neighbourhoods and remove structural defects⁸⁸. The section ‘Generative models’ discusses them in more detail, as well as their applications for sampling low-temperature glassy structures.

In physics, explaining complex behaviour builds on the ability of theories and models to substantially compress the inherent information of a natural phenomenon⁸⁹. From this standpoint, large ML models, involving hundreds or thousands of directly fitted parameters, do not qualify as a physical theory in the traditional sense of the term. Moreover, owing to their non-linearity, neural-network models are still rather difficult to interpret, although some progress is being made^{90,91}. This does not mean, however, that large ‘black-box’ ML models are useless in this context: their predictions can be instrumental as part of a heuristic process, eventually leading to a simple solution to an outstanding problem⁹². This is nicely demonstrated by the results presented in this section: building on the insight of ref. 18, the same prediction accuracy as graph neural networks was achieved using a far simpler and more transparent linear regression method²¹. Linear models, thus, retain a strong appeal for fundamental research in glass physics because of their simplicity and their direct mapping to the underlying structural descriptor. Interpreting the outcome of ML models also hinges on the ability of identifying the most relevant features, a process known as ‘feature selection’. Analysis of the so-called information imbalance has emerged as a general and elegant approach to feature selection⁹³. This method has been recently applied to identify the most relevant structural features for glassy dynamics^{94,95}.

Finally, a natural aim for future investigations is to enlarge the ML studies described above to encompass diverse glass-forming materials with complex dynamics, including active glasses as model for biological tissues^{96,97}. Although it is generally accepted that equilibrium microscopic dynamics do not influence long-time structural relaxation, it is unclear which signature activity plays on structural descriptors in active glasses⁹⁸. Similarly, very little information on the dynamical properties of glasses during ageing⁹⁹, and whether similarly strong structure–dynamics relationships can be found as for equilibrium relaxation, exists.

Learning phenomenological glass models

In this section, we demonstrate the potential of combining ML methods with physical insights to develop effective models and phenomenological theories of slow and glassy dynamics. The starting point is the ML methods, described in the previous section, that identify the local structure responsible for local relaxations on short timescales. The aim is to use this structural field as a building block to construct a phenomenological model for how structural relaxation proceeds. This approach is built upon two useful classes of models to understand dynamics in glass-forming liquids and amorphous solids subjected to mechanical strain, namely, trap and elasto-plastic models.

Trap models start from high-temperature liquid, describing the system as a distribution of energy barriers for rearrangements. One implementation¹⁰⁰ adds a facilitation mechanism: in response to a rearrangement, all the energy barriers are subject to a small random drift. This facilitated trap model has been used to explain the emergence of excess wings in the relaxation spectra¹⁰¹. Elasto-plastic models start instead from low-temperature solid, describing the system in terms of thermally induced rearrangement events that can trigger other rearrangements via long-range strain fields^{102–104}. Both of these approaches give insights into glassy dynamics and include facilitation effects in some manner, but both describe the local structure of the liquid in a very coarse-grained, simplistic manner. As a result, both classes of models must make ad hoc assumptions on the nature of the local relaxation events. In the case of the trap model, facilitation is assumed to lead to a shift of energy barriers, whereas in elasto-plastic models, the distribution of yield stress is imposed.

A recent approach unites the trap and elasto-plastic models by extending them to include the local structure in the form of a machine-learned microscopic structural descriptor, the softness S , as introduced in the previous section. Softness is sufficiently accurate that the probability of rearranging for particles of a given softness S , $P_R(S)$, has an Arrhenius temperature dependence: $P(R|S) = \exp[-\Delta E(S)/T + \Delta \Sigma(S)]$, where ΔE is the energy barrier and $\Delta \Sigma$ is the entropic one, $\Delta F = \Delta E - T\Delta \Sigma$. This temperature dependence suggests that particles of softness S have a well-defined free-energy barrier for rearrangements $\Delta F(S)$. The spatial variation of the softness then leads to a free-energy barrier field that couples to the stress and strain fields. Note that any local structural measure that predicts rearrangements or local yield stress¹⁰⁵ (whether extracted using ML, as described here or in other sections of this paper, or by other means⁸) could in principle be exploited in a similar manner to construct phenomenological models of glassy dynamics or plasticity.

Owing to this ability to extract a free-energy barrier estimate $\Delta F(S)$, the softness can naturally be used to construct a phenomenological trap model. However, softness allows one to go further by considering spatial correlations. When a rearrangement occurs, it alters the softness of the rearranging particles and that of nearby particles through near-field facilitation¹⁰⁶. It also alters the softness of more distant particles by creating a strain field that decays away from the rearrangement. Because the strain field changes the local structural environment of particles, it alters their softness. This far-field form of facilitation is well-captured by elasto-plastic models¹⁰³.

There is an interplay between rearrangements (strain), elasticity and changes in softness, with each one affecting the other two. A systematic approach to disentangling all of these effects⁷⁹ has been implemented in a lattice structuro-elasto-plasticity model²⁸ for athermal systems under load. It has been applied successfully to a number of systems of varying ductility^{28,80} and used to extract insights into the microscopic factors that control ductility, such as the strength of near-field facilitation⁸⁰.

These results pave the way towards models of structural relaxation dynamics in glassy liquids. A simple trap model, as in ref. 107, built upon the barriers $\Delta F(S)$ and assuming an underlying distribution of softness, $\rho(S)$ was developed in ref. 108. One can also construct a version of the facilitated trap model of ref. 100 that incorporates S . Generalizing such models to supercooled liquids, however, is more challenging because one must include time-reversal invariance. Above the mode-coupling temperature, T_c , near-field facilitation should be sufficient. The hypotheses that $\rho(S)$ is nearly Gaussian¹⁶ and that the near-field distribution of the change in softness $\Delta S(r)$ owing to a rearrangement at the origin is also nearly Gaussian are important simplifications that allow formulation of a closed theory¹⁰⁹. For systems below T_c , however, it has been suggested that long-range facilitation via strain occurs¹⁰⁶. The inclusion of time-reversal invariance in a model such as a thermal elasto-plastic model¹⁰³ or structuro-elasto-plasticity model with long-range facilitation is a challenging open problem that needs to be solved. A precise predictor of future dynamics, as discussed in the previous section, would be a useful tool to adjust such models. Additionally, it would be interesting to explore whether the free-energy barriers ΔF for local relaxation, extracted from the amorphous structure using softness, could be learned more directly and used to improve effective glass models.

Another path forward is to switch from a field picture to a defect picture. Most predictors of rearrangements yield particle-based quantities that are readily converted to fields, but they highlight localized regions that are susceptible to rearrangement⁸. These regions can be viewed as structural defects that interact with each other and are created and destroyed by strain and rearrangements. ML could be used to learn these interactions and rules, to help build defect theories of plasticity and glassy dynamics.

In this respect, one direction consists in letting a glass-forming liquid evolve via the usual thermal motion (using molecular dynamics (MD), for example). During such exploration, the energy is periodically minimized to extract a library of mechanically stable zero-temperature configurations (inherent structures). The idea is then to use ML to classify pairs of inherent structures, instead of single configurations, and check whether the pair is connected by a low-energy excitation corresponding to a localized structural defect. For example, a large library of inherent structures has been constructed by such an exploration at a very low temperature inside a glass basin¹¹⁰. By means of supervised learning techniques, it is possible to train a machine that takes a pair of inherent structures and provides as an output, with good precision, the classical energy barrier separating them. This strategy allowed for a speed-up in the search for glass defects by more than one order of magnitude, which is notable given the complexity of these kind of calculations.

Although this preliminary study is mostly focused on very low-energy defects that are associated with thermodynamic and transport anomalies of the glass at cryogenic temperatures¹¹⁰, it should in principle be straightforward to extend the techniques to detect other kinds of defects, such as those associated with plastic events under shear^{8,111} or relaxation events under equilibrium thermal motion¹¹². Doing so is a promising direction for further research.

Performance metrics and benchmarking

Detailed benchmarks for existing datasets, which may allow every researcher to independently develop and test new ML approaches without complex production and preprocessing of data, are essential for the development of ML techniques. We provide such benchmarks for ML glass-forming liquids for different systems, different dynamical observables and different metrics.

The benchmarks are based on the dataset GlassBench which is publicly available²⁹. The whole dataset is separated into a training set which, as the name suggests, can be used to train the neural network, and a test set which should be used only for benchmarking. In addition to initial amorphous structures and trajectories, we provide pre-calculated dynamical descriptors and propensities, as introduced in the section 'Prediction of structural relaxation and dynamic heterogeneities'. We have also uploaded a sample Python code for reading and processing. Additional technical information on the data format is provided with the dataset.

The tasks identified for GlassBench are directly related to the open questions highlighted in the 'Introduction' section. The first task is to train a model to predict single-particle propensity purely from structural properties. Accuracy is quantified using the Pearson correlation coefficient. Higher accuracy in the prediction indicates that the learned structural descriptor is indeed an important precursor for future relaxation, but it can also become essential when using the model to generate new configurations. The second task is to train a transferable model such that it can be accurately applied to different temperatures. This is an important task to enable investigation of structural relaxation at temperatures that are unreachable for numerical simulations. The third task is to train a model that correctly predicts spatial DH, as quantified by the dynamic susceptibility. The length scale of DH grows with decreasing temperature such that at very low temperatures, some regions in the system actively rearrange whereas others are completely frozen. DHs are not only important for properties of glass-forming materials but are also core to fundamental theories of the glass transition^{84,113}.

The ML techniques used for the benchmarking are summarized in Table 1. In the following section, we refer to them simply as models.

Table 1 | Overview of the different techniques benchmarked in this Technical Review

ML techniques	Training	ML approach	Free parameters	States ^a	Training time ^b	Training hardware	Application time ^c
BOTAN ²²	Supervised	GNN	54,200	th.	Hours	NVIDIA A100	Seconds
CAGE ²³	Supervised	Ridge regression	2,775	th. + cage	Minutes	CPU	Hours
GlassMLP ²⁷	Supervised	MLP	615	th. + inh.	Minutes	CPU	Seconds
SE(3) ²⁵	Supervised	GNN	52,660	th. + inh.	Hours	NVIDIA Tesla V100	Seconds
SBO ⁴⁹	Unsupervised	PCA	0	th.	NA	CPU	Seconds

CPU, central processing unit; GNN, graph neural network; inh., inherent; ML, machine learning; MLP, multilayer perceptron; NA, not applicable; PCA, principle component analysis; th., thermal. ^aUsage of thermal, inherent or cage states. ^bTime required to train one model at a specific temperature and time for the Kob-Andersen system in 3D. ^cTime required to calculate the prediction for a single configuration, including preparation such as calculation of inh. or cage states.

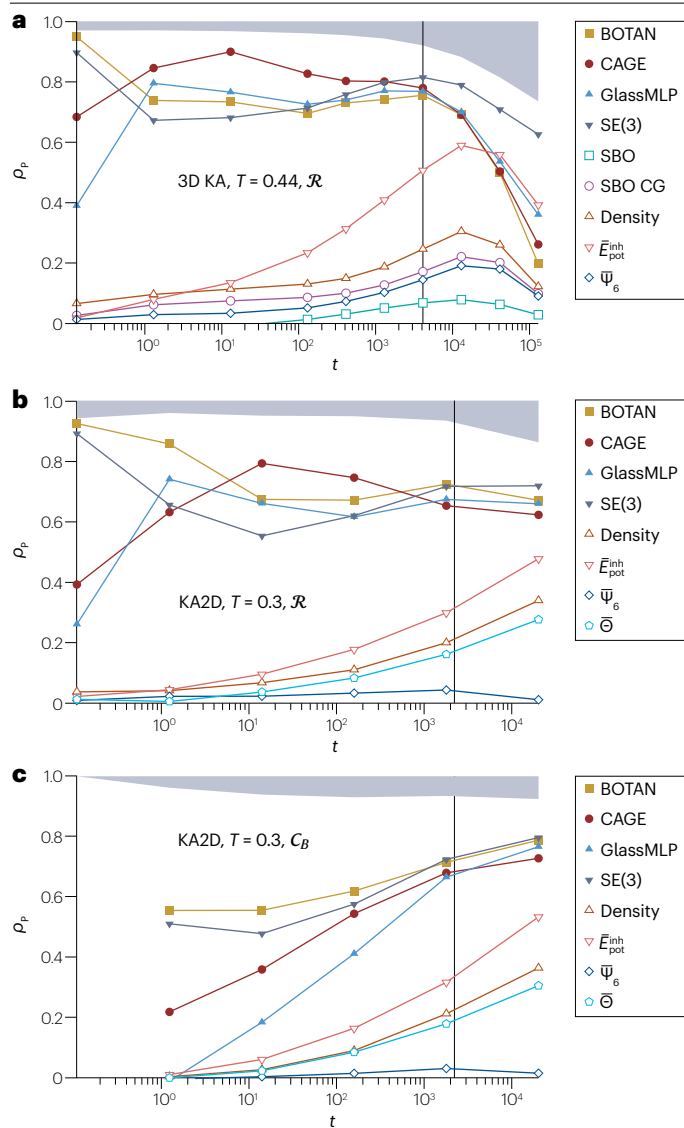


Fig. 4 | Training a model to predict single-particle propensity purely from structural properties. Pearson correlation ρ_p between various structural indicators with the ground truth. **a.** Three-dimensional Kob–Andersen (KA) model at dimensionless temperature $T = 0.44$. **b, c.** Two-dimensional KA (KA2D) systems at $T = 0.3$. The dynamical variable in parts **a** and **b** is the propensity of displacements \mathcal{R} , and in part **c**, it is the bond-breaking propensity \mathcal{C}_B . Full symbols corresponding to supervised machine learning techniques and open symbols to unsupervised techniques or physically motivated structural descriptors. The vertical line marks the structural relaxation time τ_α , the typical timescale on which particles rearrange, as defined in equation (1) in the Supplementary information. The exclusion zone on the top (grey-shaded region) marks the highest achievable correlation given the finite number of replicas.

A large variety of different models is represented, with very different numbers of fitting parameters and training time. Furthermore, the models use various ways to physically pre-process the structural input, either by using inherent states²⁷ or even by performing a Monte Carlo averaging of local cages²³. These different factors, combined with

the benchmarking provided below, should help in choosing the most suitable method for a given purpose, with focus on either the highest-scoring predictions, computational efficiency, or interpretability. In addition to these ML techniques, we also include the performance of traditional structural descriptors based on physical intuition^{6,27,114}. The model of glass-forming liquid that we selected to develop GlassBench is the very popular KA mixture, which we study both in 2D and 3D.

Training a model to predict single-particle propensity purely from structural properties

The aim for the models is to learn correlations between the amorphous structure and the dynamic propensity of displacements, $\mathcal{R}_i(t) \equiv \langle |\Delta \mathbf{r}_i(t)| \rangle_{\text{iso}}$, as introduced in the section ‘Prediction of structural relaxation and dynamic heterogeneities’. A common metric used to assess the performance of different techniques is the Pearson correlation coefficient:

$$\rho_p = \frac{\text{cov}(\mathcal{R}_i^{\text{MD}}, \mathcal{X}_i^{\text{ML}})}{\sqrt{\text{var}(\mathcal{R}_i^{\text{MD}})\text{var}(\mathcal{X}_i^{\text{ML}})}}, \quad (1)$$

between the labels $\mathcal{R}_i^{\text{MD}}$ for each particle i of type 1 in the entire dataset as obtained from MD simulations, and the ML output $\mathcal{X}_i^{\text{ML}}$. (Calculating the Pearson correlation for each structure individually and then averaging yields slightly different results, and Pearson correlations appear to be systematically higher. Similarly, calculating Pearson correlation over particles of different type significantly increases the correlation, and this should be avoided.) The results are shown in Fig. 4a. All technical details are provided in the Supplementary information. Supervised techniques nearly approach the maximal achievable correlation over the entire range of timescales. CAGE performs best for shorter times, which appears reasonable because it uses extensive Monte Carlo simulations to characterize the local cage structure at short times. For longer times, the SE(3) GNN extension has the strongest correlation, closely trailed by the other advanced techniques. There is a pronounced gap between the supervised and the unsupervised techniques, indicating that the amorphous structural features that are predictive for dynamics do not stand out in a purely structural analysis, as discussed in the section ‘Machine learning locally favoured structures’.

The generality of these findings is seen in benchmarks for a 2D ternary mixture of Lennard–Jones particles (KA2D) (Fig. 4b). Apart from minor differences, the performance of the individual techniques is very similar to a 3D system. The most noteworthy difference is perhaps that BOTAN performs best of all methods at the structural relaxation time $t \approx \tau_\alpha$, whereas in a 3D KA system, the trend is reversed. Although there might be subtle differences between structural relaxation across spatial dimensions, the above observation implies that the problem of learning correlations between structure and dynamics is essentially independent of the spatial dimension.

The propensity of displacements \mathcal{R}_i is only one choice of how to characterize relaxation dynamics, among many others. One alternative is to use the bond-breaking correlation, \mathcal{C}_B^i , which quantifies how many nearest neighbours are lost by particle i during the relaxation process^{27,112}. The models also successfully learn correlations between the bond-breaking propensity and the amorphous structure (Fig. 4c). However, the performance of the models in the short-time predictions is substantially reduced compared to the propensity of displacements. This suggests that predicting the exact nature and position of the first

rearrangement events is more difficult than simply predicting short-time displacements. Around the structural relaxation time τ_α and beyond, the correlations shown in Fig. 4c for C_B^i are stronger than for \mathcal{R}_i in Fig. 4b. This seemingly surprising result is connected to the growing DH at longer times, which simplifies the prediction of larger rearranging clusters from coarse-grained structural properties²⁷. Additionally, at times $t \geq \tau_\alpha$, the propensity of displacement \mathcal{R}_i has slowly decaying tails which are not captured by the models (see Supplementary Fig. 2) and, thus, probably reduce the Pearson correlation.

Training a transferable model across different temperatures

With the goal of predicting the dynamics at very low temperatures that are inaccessible by direct computer simulations, an important property of supervised ML techniques is their transferability, in particular towards lower temperatures^{25,83}. In Fig. 5, we show the capabilities of the models to transfer the structure–dynamics relationships they learned at a given temperature to make predictions at a different temperature. The results are actually quite remarkable because transferability is generically quite good for all models. This shows that these relationships evolve smoothly across the range of temperatures investigated here. In particular, the models trained at $1/T = 2.0$ ($\tau_\alpha = 210$) perform nearly as well in predicting propensity at $1/T = 2.25$ ($\tau_\alpha = 4,100$) as the models trained directly at $1/T = 2.25$. The SE(3) method seems to be particularly suited to transfer to lower temperatures, opening the possibility to study structural relaxation at much lower temperatures.

Training a model that correctly predicts spatial DH

Finally, we investigate the performance of the models to predict the correct extent of DH. A time-dependent scalar variable that quantifies heterogeneities is the dynamic susceptibility

$$\chi_4(t) = N \left(\langle \bar{C}_R^2(t) \rangle - \langle \bar{C}_R(t) \rangle^2 \right) \quad (2)$$

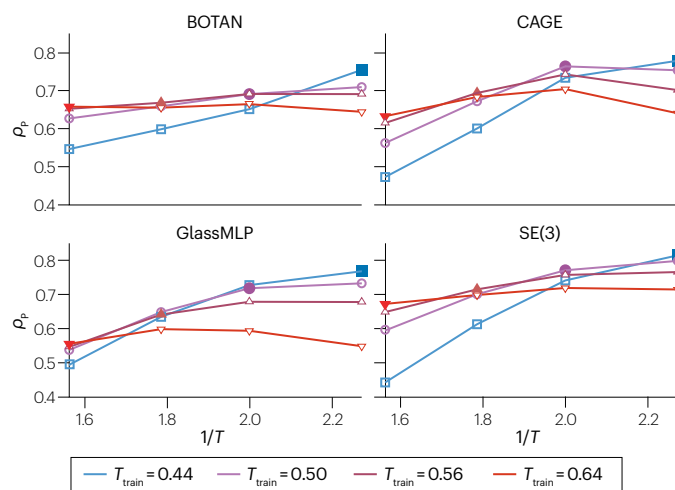


Fig. 5 | Training a transferable model to be accurate at different temperatures. Transferability in temperature T of trained networks in the Kob–Andersen (KA) system (3D) at the structural relaxation time τ_α . Each network is trained at T_{train} (filled symbols) and applied to all four different temperatures (open symbols). Colours indicate smooth T_{train} transition from high temperature (red, $T = 0.64$) to low temperature (blue, $T = 0.44$).

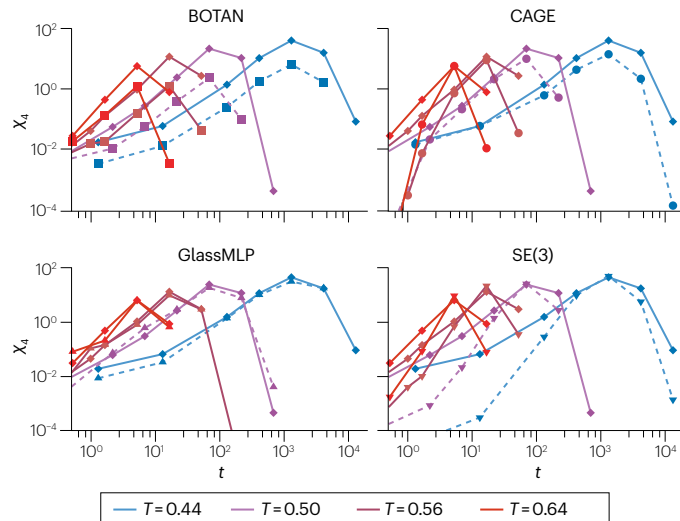


Fig. 6 | Training a model that correctly predicts spatial dynamic heterogeneity. Dynamic susceptibility $\chi_4(t)$ for different temperatures ($T = 0.44, 0.5, 0.56$ and 0.64), as predicted from machine learning techniques (dashed lines), compared to the ground truth (full lines) in the Kob–Andersen system (3D). The colour code is the same as that in Fig. 5.

calculated from the system-averaged overlap function $\bar{C}_R(t) = (1/N) \sum_{i \in N} \Theta(0.3 - \mathcal{R}_i(t))$. Here, N is the number of particles in the system, and $\Theta(x)$ is the Heaviside function. This definition separates particles into active ($\mathcal{R}_i > 0.3$) and frozen ($\mathcal{R}_i \leq 0.3$). The threshold value of 0.3 is a common choice^{115,116} and corresponds to values slightly larger than the plateau in the mean-squared displacement¹¹⁵, implying that particles identified as active have typically left their initial cages. In Fig. 6, we compare the results of the predictions to the ground truth MD simulations. Despite the overall good performance in the Pearson correlation, there are strong differences between the various techniques. For example, the improvement in performance of SE(3) compared to BOTAN (Fig. 4) can be connected to their different learning of the correct DH. In an attention-based GNN extension, this heterogeneity was explicitly targeted during the training procedure to improve the performance of the deep network¹¹⁷. The best overall performance in predicting $\chi_4(t)$ is achieved by GlassMLP, which was specifically constructed to learn and predict DH²⁷. This analysis shows that the Pearson correlation is not entirely sufficient to quantify the performance of a model. Additional dynamical observables, such as the dynamic susceptibility $\chi_4(t)$, should be investigated to better characterize the ability of models to realistically describe structural relaxation in glass-forming liquids.

Other benchmarks and possible extensions

In the Supplementary information, we provide further benchmarking by investigating the following: the coefficient of determination R^2 , another popular measure to study the performance of ML models; the probability distributions of the predicted propensities, which correspond to a second contribution to DH; the scatter plots and the snapshots directly comparing the true and predicted propensities; the cross-correlations between the different structural descriptors and the models investigated in this section. We also provide additional information on learning curves, transferability to lower temperatures $T = 0.4$, and bond-breaking propensity.

Another conclusion of additional benchmarks, which goes beyond our scope here, is that correlation coefficients display some system dependence⁶⁸. Hard sphere glasses and systems with strong icosahedral order, for example, show systematically higher correlation coefficients between structural and dynamical descriptors than Kob–Andersen mixtures do^{21,49}. The same statement holds true for different dynamical descriptors and coarse-grained quantities. We, therefore, strongly encourage the use of identical datasets and labels (that is, dynamical descriptors) to enable comparability.

Among possible extensions of GlassBench, it would be particularly worth including a diverse set of models of glass formers: fragile molecular glass formers, strong network-forming glasses and metallic glasses. The first step in creating a new dataset is the sampling of independent configurations at a given temperature or density. This step could leverage enhanced sampling techniques such as parallel tempering¹¹⁸ or swap Monte Carlo¹¹⁹. Subsequently, for each structure, molecular dynamics or ab-initio dynamics simulations need to be performed to study the structural relaxation of the systems and calculate the isoconfigurational average⁸¹.

It would also be interesting to broaden the tasks. For example, other ML models, such as the softness derived from SVC, target predicting local energy barriers for short-time rearrangements instead of long-time structural relaxation^{16,79} (see the section ‘Learning phenomenological glass models’). For this class of ML techniques, it would be preferable that the descriptor efficiently separates the particles by their probability of rearrangement, $P_R(S)$. To encourage further development in this area, it would be desirable to perform similar benchmarking and investigate whether modern ML models can outperform the state of the art.

Similarly, there is much interest in understanding plastic events and failure of glassy materials under external load. Unlike equilibrium structural relaxation, this protocol takes place far from equilibrium, but it displays similar characteristics. A few years ago, this field has been reviewed and benchmarked in a collaborative publication⁸. The focus, however, was not yet on advanced ML techniques – which further demonstrates the rapid development of this field. It would be interesting to analyse whether the techniques presented in this Technical Review can help in investigating glass deformation under shear^{18,120–122}.

Outlook

Potential applications of ML techniques for studies of glass-forming liquids and glasses go beyond what we covered in this article, focusing on fundamental aspects of glassy dynamics. Directions include investigation of specific material properties^{65,66,123,124} or material discovery^{63,125,126}, machine learning force fields¹²⁷ and particle identification in experimental data^{128,129}. Furthermore, the connection between ML and glassy physics has also gone in the reverse direction, by borrowing methods developed for the study of disordered systems to analyse central theoretical ML problems. In fact, the connection between the rough energy landscape of amorphous materials and optimization defined by loss functions with many local minima has been used to better understand and optimize learning of neural networks^{37,130–134}.

We anticipate that ML will continue to impact glass research and lead to the development of new major directions in the field. We close this Technical Review by discussing exciting new concepts that have the potential to play an important part in future research.

Attention and transformers

An important advance in ML architectures is the ‘attention mechanism’¹³⁵. Using it in ML methods for glassy dynamics has a lot of

potential. The fundamental concept behind attention is to assign a learnable level of importance to specific parts of the input or intermediate representation. This could be distinct words in sentences (see, for instance, ChatGPT), specific features of amorphous structures, channels in a deep representation or neighbouring atoms in a graph representation. Broadly speaking, this can be achieved by making learned weights themselves dependent on the input.

Examples of successful applications of attention are AlphaFold v2 and RoseTTAFold^{136,137}, which both use a rotation-equivariant attention-based transformer to predict the 3D structure of proteins. This architecture differs from the graph network architectures discussed earlier by the dense character of its computation mechanism: all atoms in the input can exchange information with all other atoms (with a learned modulation as a function of the distance), allowing for a more flexible computation. Variants of these architectures tend to obtain results that are competitive with sparse graph networks on benchmark tasks¹³⁸. A network with a self-attention mechanism has been developed for predicting glassy dynamics¹¹⁷, and it shows that the curse of overfitting can be avoided. The broader concept of input-dependent weights was also used in a similar context to learn DH over a wide range of temperatures at which attention must be paid to temperature-dependent length scales⁸³. Both of the approaches are, however, rather direct applications of the idea of positional encoding for learning attention weights, and more complex networks, such as full-fledged transformers¹³⁵, are expected to be used in future research.

Going in the opposite direction from transformers, attention mechanisms can also be used to make models more interpretable. For example, they can help identify the task-relevant sectors in the input data⁹¹. Additionally, attention can also be incorporated into other architectures, for example, in combination with a temporal encoding in time-series forecasting¹³⁹, to identify relevant parts of past trajectories.

Self-supervised, semi-supervised and reinforcement learning

We have mainly focused on ‘traditional’ unsupervised and supervised learning techniques because they are better established in the field. However, there are several other learning paradigms that may be useful for future projects, some of which have started to be used in glass research.

To learn the connection between structural order and structural relaxation in a way that reconciles the unsupervised and supervised approaches, a possibility is to use semi-supervised learning¹⁴⁰. Concretely, the idea is to perform self-supervised learning using only unlabelled input configurations by designing a pretext task, such as reinserting a particle which has been artificially removed from a configuration, de-noising positions of particles, or predicting local quantities (such as the potential energy of each particle or its distance to its quenched position)⁸⁵. Once a representation has been learned to perform this mock task, one can fine-tune only a handful of parameters to correlate the learned representation to the relevant dynamical variable. Such self-supervised pre-training has proven effective in increasing performance for various downstream tasks that are similar in spirit to glassy dynamics prediction, such as the prediction of molecular properties¹⁴¹, crystalline material properties¹⁴² or organic semiconductors optoelectronic properties¹⁴³.

In the application to glasses, the key element of this approach is to build most of the network without looking at labels, so the output of such a method may be more acceptable as a bona fide structural descriptor, as opposed to heavy networks relying purely on supervised learning. Additionally, it requires fewer labelled data which becomes

very important at low temperatures at which sampling becomes difficult. The described methodology could, therefore, also be used to improve transferability of pre-trained models.

Although reinforcement learning is a well-established tool in the field of ML¹⁴⁴, it has found applications in physics for improved sampling^{145,146} or structure optimization^{147,148} only very recently. The general idea behind reinforcement learning is to learn to take specific actions when reaching certain states. The goal is to find the policy of actions leading to optimal results, as quantified by a reward function. Applying this approach to the example of searching ground states in spin glasses, the state would be the observed structure, the action would be a spin flip, and the reward would be the energy change after several spin flips¹⁴⁶. Along these lines, the Metropolis–Hastings algorithm has been formulated in a reinforcement learning setting suitable for simulations of spin systems¹⁴⁹. This approach has been extended to learn new Monte Carlo moves that accelerate sampling of supercooled liquids¹⁵⁰, establishing connections with related adaptive Monte Carlo methods^{151,152}. One of the goals of this line of research is to improve and generalize the swap Monte Carlo algorithm, which demonstrated an impressive performance for specifically adapted glass models^{119,153} and has led to a series of insights into supercooled liquids^{101,112}. Devising general-purpose enhanced sampling algorithms to simulate glassy systems represents an exciting challenge for future research¹⁵⁴.

Generative models

Another promising emerging direction for applying ML techniques to problems relevant to fundamental aspects of glass physics is the use of generative models (GMs). One of the key problems in theoretical studies of glassy dynamics is that of sampling. In fact, for systems exhibiting glassy dynamics, it is very challenging to efficiently sample configurations x_i from a Gibbs distribution of the form $P(x_i) = \exp[-\beta U(x_i)]/Z$, where $\beta^{-1} = k_B T$ is the target inverse temperature and $U(x_i)$ is the known potential energy. Unlike the generative modelling of images, in which one estimates an unknown probability distribution from data, here the target distribution is known from the start, and sampling from it is the challenge.

Two early lines of research were proposed independently, one known as Boltzmann generators¹⁵⁵ and one based on variational autoregressive networks¹⁵⁶. The idea is to consider a much simpler distribution $\tilde{P}(z)$ such that one can easily sample z_i in a single shot. This can, for example, be a Gaussian model, an autoregressive model or a Gibbs distribution at very high temperatures at which one can sample efficiently. After learning, independent samples x can then be generated using the invertible map $x_i = f(z_i)$ of the model. Computing the biased distribution $P_{GM}(x)$ of the generative model enables unbiasing x_i in a last post-processing step¹⁵⁵. This ensures that the samples are exactly drawn from the distribution $P(x)$.

In practice, the method is only efficient if the weights are almost uniformly distributed. This requires that the generative distribution is as close as possible to the target distribution. To this aim, the machine is trained to minimize the Kullback–Leibler (KL) divergence between the generative and target distributions. Because the KL divergence between two distributions is not symmetric, two choices can be made. One choice is maximum likelihood training, in which one minimizes $D_{KL}(P||P_{GM})$. This approach has the advantage that P_{GM} has to cover well all the support of $P(x)$. However, it also requires existing samples from $P(x)$, which renders training impractical: to train a machine to sample from the target requires being able to sample from the target. The other choice is variational or energy-based training, in which one

minimizes $D_{KL}(P_{GM}||P)$, which corresponds to the free energy of the generative model. Although this choice does not require sampling from P_{GM} , it has the important drawback that the generative model might only cover part of the support of the target, a limitation known as mode collapse.

To deal with these problems, several architectures and training strategies have been proposed. To sample a two-state protein model, a normalizing flow architecture was used to represent the map $f(z)$, and a training strategy was developed based on mixing the variational approach with maximum likelihood, for which experimental structures and short molecular dynamics simulations were used¹⁵⁵. In a subsequent work, equivariant flows were used to implement physical symmetries¹⁵⁷, and a higher-temperature Boltzmann distribution was used as a prior distribution^{158,159} (see also refs. 160,161). To sample crystalline structures, it has been proposed to generate displacements from a reference lattice structure instead of absolute particle positions¹⁶². A more efficient training strategy is based on mixing standard Monte Carlo moves with moves proposed by the generative model¹⁵². Applying Boltzmann generators to sample supercooled liquids yields performances in the same magnitude as those of previously known enhanced sampling techniques¹⁶³.

Several studies have focused on other models in which sampling is challenging, such as spin glasses, hard optimization problems and lattice field theories^{146,156,164–176}. How these methods compare to standard ones and whether the efficiency is universal or model dependent remain unclear^{177–180}.

Finally, it could be worth combining the ML models discussed in the section ‘Prediction of structural relaxation and dynamic heterogeneities’, which can precisely predict future dynamics, with generative models. The former can be used to detect active regions or even particles which tend to rearrange, and the latter can subsequently propose new configurations based on local rearrangements.

Data availability

The dataset GlassBench and Python scripts used to create the benchmarks presented in the section ‘Performance metrics and benchmarking’ are publicly available and can be downloaded from Zenodo at <https://doi.org/10.5281/zenodo.10118191> (ref. 29).

Published online: 6 January 2025

References

1. Ediger, M. D., Angell, C. A. & Nagel, S. R. Supercooled liquids and glasses. *J. Phys. Chem.* **100**, 13200–13212 (1996).
2. Cavagna, A. Supercooled liquids for pedestrians. *Phys. Rep.* **476**, 51–124 (2009).
3. LeCun, Y., Bengio, Y. & Hinton, G. Deep learning. *Nature* **521**, 436–444 (2015).
4. Alzubaidi, L. et al. Review of deep learning: concepts, CNN architectures, challenges, applications, future directions. *J. Big Data* **8**, 1–74 (2021).
5. Royall, C. P. & Williams, S. R. The role of local structure in dynamical arrest. *Phys. Rep.* **560**, 1–75 (2015).
6. Tanaka, H., Tong, H., Shi, R. & Russo, J. Revealing key structural features hidden in liquids and glasses. *Nat. Rev. Phys.* **1**, 333–348 (2019).
7. Marin-Aguilar, S., Wensink, H. H., Foffi, G. & Smallegang, F. Tetrahedrality dictates dynamics in hard sphere mixtures. *Phys. Rev. Lett.* **124**, 208005 (2020).
8. Richard, D. et al. Predicting plasticity in disordered solids from structural indicators. *Phys. Rev. Mater.* **4**, 113609 (2020).
9. Boattini, E. et al. Autonomously revealing hidden local structures in supercooled liquids. *Nat. Commun.* **11**, 5479 (2020).
10. Paret, J., Jack, R. L. & Coslovich, D. Assessing the structural heterogeneity of supercooled liquids through community inference. *J. Chem. Phys.* **152**, 144502 (2020).
11. Oyama, N., Koyama, S. & Kawasaki, T. What do deep neural networks find in disordered structures of glasses? *Front. Phys.* **10**, 1320 (2023).
12. Soltani, S., Sinclair, C. W. & Rottler, J. Exploring glassy dynamics with Markov state models from graph dynamical neural networks. *Phys. Rev. E* **106**, 025308 (2022).

13. Widmer-Cooper, A. & Harrowell, P. Predicting the long-time dynamic heterogeneity in a supercooled liquid on the basis of short-time heterogeneities. *Phys. Rev. Lett.* **96**, 185701 (2006).
14. Widmer-Cooper, A., Perry, H., Harrowell, P. & Reichman, D. R. Irreversible reorganization in a supercooled liquid originates from localized soft modes. *Nat. Phys.* **4**, 711–715 (2008).
15. Berthier, L. & Biroli, G. Theoretical perspective on the glass transition and amorphous materials. *Rev. Mod. Phys.* **83**, 587–645 (2011).
16. Schoenholz, S. S., Cubuk, E. D., Sussman, D. M., Kaxiras, E. & Liu, A. J. A structural approach to relaxation in glassy liquids. *Nat. Phys.* **12**, 469–471 (2016).
17. Cubuk, E. D. et al. Identifying structural flow defects in disordered solids using machine-learning methods. *Phys. Rev. Lett.* **114**, 108001 (2015).
18. Bapst, V. et al. Unveiling the predictive power of static structure in glassy systems. *Nat. Phys.* **16**, 448–454 (2020).
19. Yang, Z.-Y., Wei, D., Zacccone, A. & Wang, Y.-J. Machine-learning integrated glassy defect from an intricate configurational-thermodynamic-dynamic space. *Phys. Rev. B* **104**, 064108 (2021).
20. Boattini, E., Smalenburg, F. & Filion, L. Averaging local structure to predict the dynamic propensity in supercooled liquids. *Phys. Rev. Lett.* **127**, 088007 (2021).
21. Alkemade, R. M., Boattini, E., Filion, L. & Smalenburg, F. Comparing machine learning techniques for predicting glassy dynamics. *J. Chem. Phys.* **156**, 204503 (2022).
22. Shiba, H., Hanai, M., Suzumura, T. & Shimokawabe, T. BOTAN: BOnd Targeting Network for prediction of slow glassy dynamics by machine learning relative motion. *J. Chem. Phys.* **158**, 084503 (2023).
23. Alkemade, R. M., Smalenburg, F. & Filion, L. Improving the prediction of glassy dynamics by pinpointing the local cage. *J. Chem. Phys.* **158**, 134512 (2023).
24. Ciarella, S., Chiappini, M., Boattini, E., Dijkstra, M. & Janssen, L. M. C. Dynamics of supercooled liquids from static averaged quantities using machine learning. *Mach. Learn. Sci. Technol.* **4**, 025010 (2023).
25. Pezzicoli, F. S., Charpiat, G. & Landes, F. P. Rotation-equivariant graph neural networks for learning glassy liquids representations. *SciPost Phys.* **16**, 136 (2024).
26. Ruiz-Garcia, M. et al. Discovering dynamic laws from observations: the case of self-propelled, interacting colloids. *Phys. Rev. E* **109**, 064611 (2024).
27. Jung, G., Biroli, G. & Berthier, L. Predicting dynamic heterogeneity in glass-forming liquids by physics-inspired machine learning. *Phys. Rev. Lett.* **130**, 238202 (2023).
28. Zhang, G. et al. Structuro-elasto-plasticity model for large deformation of disordered solids. *Phys. Rev. Res.* **4**, 043026 (2022).
29. Jung, G. GlassBench. zenodo <https://doi.org/10.5281/zenodo.10118191> (2023).
30. Kob, W. & Andersen, H. C. Testing mode-coupling theory for a supercooled binary Lennard-Jones mixture I: the van Hove correlation function. *Phys. Rev. E* **51**, 4626–4641 (1995).
31. Tarjus, G., Kivelson, D. & Viot, P. The viscous slowing down of supercooled liquids as a temperature-controlled super-Arrhenius activated process: a description in terms of frustration-limited domains. *J. Phys. Condens. Matter* **12**, 6497 (2000).
32. Tanemura, M. et al. Geometrical analysis of crystallization of the soft-core model. *Prog. Theor. Phys.* **58**, 1079–1095 (1977).
33. Malins, A., Williams, S. R., Eggers, J. & Royall, C. P. Identification of structure in condensed matter with the topological cluster classification. *J. Chem. Phys.* **139**, 234506 (2013).
34. Honeycutt, J. D. & Andersen, H. C. Molecular dynamics study of melting and freezing of small Lennard-Jones clusters. *J. Phys. Chem.* **91**, 4950–4963 (1987).
35. Lazar, E. A., Han, J. & Srolovitz, D. J. A topological framework for local structure analysis in condensed matter. *Proc. Natl Acad. Sci. USA* **112**, E5769–E5776 (2015).
36. Steinhart, P. J., Nelson, D. R. & Ronchetti, M. Bond-orientational order in liquids and glasses. *Phys. Rev. B* **28**, 784–805 (1983).
37. Mehta, P. et al. A high-bias, low-variance introduction to machine learning for physicists. *Phys. Rep.* **810**, 1–124 (2019).
38. Cheng, B. et al. Mapping materials and molecules. *Acc. Chem. Res.* **53**, 1981–1991 (2020).
39. Glielmo, A. et al. Unsupervised learning methods for molecular simulation data. *Chem. Rev.* **121**, 9722–9758 (2021).
40. Jarry, P. & Jakse, N. Medium range ordering in liquid Al-based alloys: towards a machine learning approach of solidification. *IOP Conf. Ser. Mater. Sci. Eng.* **1274**, 012001 (2023).
41. Hu, W., Singh, R. R. P. & Scalettar, R. T. Discovering phases, phase transitions, and crossovers through unsupervised machine learning: a critical examination. *Phys. Rev. E* **95**, 062122 (2017).
42. Rodriguez-Nieva, J. F. & Scheurer, M. S. Identifying topological order through unsupervised machine learning. *Nat. Phys.* **15**, 790–795 (2019).
43. Mendes-Santos, T., Turkeshi, X., Dalmon, M. & Rodriguez, A. Unsupervised learning universal critical behavior via the intrinsic dimension. *Phys. Rev. X* **11**, 011040 (2021).
44. Bartók, A. P., Kondor, R. & Csányi, G. On representing chemical environments. *Phys. Rev. B* **87**, 184115 (2013).
45. Parsaeifard, B. et al. An assessment of the structural resolution of various fingerprints commonly used in machine learning. *Mach. Learn. Sci. Technol.* **2**, 015018 (2021).
46. Midtvedt, B. et al. Single-shot self-supervised object detection in microscopy. *Nat. Commun.* **13**, 7492 (2022).
47. Caro, M. A., Deringer, V. L., Koskinen, J., Laurila, T. & Csányi, G. Growth mechanism and origin of high sp^3 in tetrahedral amorphous carbon. *Phys. Rev. Lett.* **120**, 166101 (2018).
48. Monserrat, B., Brandenburg, J. G., Engel, E. A. & Cheng, B. Liquid water contains the building blocks of diverse ice phases. *Nat. Commun.* **11**, 5757 (2020).
49. Coslovich, D., Jack, R. L. & Paret, J. Dimensionality reduction of local structure in glassy binary mixtures. *J. Chem. Phys.* **157**, 204503 (2022).
50. Banerjee, A., Hsu, H.-P., Kremer, K. & Kukhareenko, O. Data-driven identification and analysis of the glass transition in polymer melts. *ACS Macro Lett.* **12**, 679–684 (2023).
51. Banerjee, A., Iscen, A., Kremer, K. & Kukhareenko, O. Determining glass transition in all-atom acrylic polymeric melt simulations using machine learning. *J. Chem. Phys.* **159**, 074108 (2023).
52. Offei-Danso, A., Hassanali, A. & Rodriguez, A. High-dimensional fluctuations in liquid water: combining chemical intuition with unsupervised learning. *J. Chem. Theory Comput.* **18**, 3136–3150 (2022).
53. Campadelli, P., Casiraghi, E., Ceruti, C. & Rozza, A. Intrinsic dimension estimation: relevant techniques and a benchmark framework. *Math. Probl. Eng.* **2015**, e759567 (2015).
54. Parsaeifard, B. & Goedecker, S. Manifolds of quasi-constant SOAP and ACSF fingerprints and the resulting failure to machine learn four-body interactions. *J. Chem. Phys.* **156**, 034302 (2022).
55. Darby, J. P., Kermode, J. R. & Csányi, G. Compressing local atomic neighbourhood descriptors. *npj Comput. Mater.* **8**, 1–13 (2022).
56. Darby, J. P. et al. Tensor-reduced atomic density representations. *Phys. Rev. Lett.* **131**, 028001 (2023).
57. Coslovich, D., Ozawa, M. & Berthier, L. Local order and crystallization of dense polydisperse hard spheres. *J. Phys. Condens. Matter* **30**, 144004 (2018).
58. Tong, H. & Tanaka, H. Emerging exotic compositional order on approaching low-temperature equilibrium glasses. *Nat. Commun.* **14**, 4614 (2023).
59. Elliott, S. R. Medium-range structural order in covalent amorphous solids. *Nature* **354**, 445–452 (1991).
60. Sheg, H., Luo, W., Alamgir, F., Bai, J. & Ma, E. Atomic packing and short-to-medium-range order in metallic glasses. *Nature* **439**, 419–425 (2006).
61. Montes de Oca, J. M., Sciortino, F. & Appignanesi, G. A structural indicator for water built upon potential energy considerations. *J. Chem. Phys.* **152**, 244503 (2020).
62. Faccio, C., Benzi, M., Zanetti-Polzi, L. & Daidone, I. Low- and high-density forms of liquid water revealed by a new medium-range order descriptor. *J. Mol. Liq.* **355**, 118922 (2022).
63. Mauro, J. C., Tandia, A., Vargheese, K. D., Mauro, Y. Z. & Smedskjaer, M. M. Accelerating the design of functional glasses through modeling. *Chem. Mater.* **28**, 4267–4277 (2016).
64. Cassar, D. R. et al. Predicting and interpreting oxide glass properties by machine learning using large datasets. *Ceram. Int.* **47**, 23958–23972 (2021).
65. Bødker, M. L., Bauchy, M., Du, T., Mauro, J. C. & Smedskjaer, M. M. Predicting glass structure by physics-informed machine learning. *npj Comput. Mater.* **8**, 192 (2022).
66. Bhattoo, R. et al. Artificial intelligence and machine learning in glass science and technology: 21 challenges for the 21st century. *Int. J. Appl. Glass Sci.* **12**, 277–292 (2021).
67. Doliwa, B. & Heuer, A. What does the potential energy landscape tell us about the dynamics of supercooled liquids and glasses? *Phys. Rev. Lett.* **91**, 235501 (2003).
68. Hocky, G. M., Coslovich, D., Ikeda, A. & Reichman, D. R. Correlation of local order with particle mobility in supercooled liquids is highly system dependent. *Phys. Rev. Lett.* **113**, 157801 (2014).
69. Tong, H. & Tanaka, H. Revealing hidden structural order controlling both fast and slow glassy dynamics in supercooled liquids. *Phys. Rev. X* **8**, 011041 (2018).
70. Schoenholz, S. S., Cubuk, E. D., Kaxiras, E. & Liu, A. J. Relationship between local structure and relaxation in out-of-equilibrium glassy systems. *Proc. Natl Acad. Sci. USA* **114**, 263–267 (2017).
71. Sussman, D. M., Schoenholz, S. S., Cubuk, E. D. & Liu, A. J. Disconnecting structure and dynamics in glassy thin films. *Proc. Natl Acad. Sci. USA* **114**, 10601–10605 (2017).
72. Cubuk, E. D. et al. Structure-property relationships from universal signatures of plasticity in disordered solids. *Science* **358**, 1033–1037 (2017).
73. Harrington, M., Liu, A. J. & Durian, D. J. Machine learning characterization of structural defects in amorphous packings of dimers and ellipses. *Phys. Rev. E* **99**, 022903 (2019).
74. Ma, X. et al. Heterogeneous activation, local structure, and softness in supercooled colloidal liquids. *Phys. Rev. Lett.* **122**, 028001 (2019).
75. Cubuk, E. D., Liu, A. J., Kaxiras, E. & Schoenholz, S. S. Unifying framework for strong and fragile liquids via machine learning: a study of liquid silica. Preprint at <https://doi.org/10.48550/arXiv.2008.09681> (2020).
76. Ridout, S. A., Rocks, J. W. & Liu, A. J. Correlation of plastic events with local structure in jammed packings across spatial dimensions. *Proc. Natl Acad. Sci. USA* **119**, e2119006119 (2022).
77. Tah, I., Ridout, S. A., & Liu, A. J. Fragility in glassy liquids: a structural approach based on machine learning. *J. Chem. Phys.* **157**, 124501 (2022).
78. Liu, H., Smedskjaer, M. M. & Bauchy, M. Deciphering a structural signature of glass dynamics by machine learning. *Phys. Rev. B* **106**, 214206 (2022).
79. Zhang, G., Ridout, S. A. & Liu, A. J. Interplay of rearrangements, strain, and local structure during avalanche propagation. *Phys. Rev. X* **11**, 041019 (2021).
80. Xiao, H. et al. Machine learning-informed structuro-elastoplasticity predicts ductility of disordered solids. Preprint at <https://doi.org/10.48550/arXiv.2303.12486> (2023).
81. Widmer-Cooper, A., Harrowell, P. & Fynewever, H. How reproducible are dynamic heterogeneities in a supercooled liquid? *Phys. Rev. Lett.* **93**, 135701 (2004).
82. Berthier, L. & Jack, R. L. Structure and dynamics of glass formers: predictability at large length scales. *Phys. Rev. E* **76**, 041509 (2007).
83. Jung, G., Biroli, G. & Berthier, L. Dynamic heterogeneity at the experimental glass transition predicted by transferable machine learning. *Phys. Rev. B* **109**, 064205 (2024).
84. Berthier, L., Biroli, G., Bouchaud, J.-P., Cipelletti, L. & Saarloos, W. *Dynamical Heterogeneities in Glasses, Colloids, and Granular Media* (Oxford Univ. Press, 2011).

85. Gidaris, S., Singh, P. & Komodakis, N. Unsupervised representation learning by predicting image rotations. Preprint at <https://doi.org/10.48550/arXiv.1803.07728> (2018).
86. Toninelli, C., Wyart, M., Berthier, L., Biroli, G. & Bouchaud, J.-P. Dynamical susceptibility of glass formers: contrasting the predictions of theoretical scenarios. *Phys. Rev. E* **71**, 041505 (2005).
87. Kingma, D. P. et al. An introduction to variational autoencoders. *Found. Trends Mach. Learn.* **12**, 307–392 (2019).
88. Wang, Q. & Zhang, L. Inverse design of glass structure with deep graph neural networks. *Nat. Commun.* **12**, 5359 (2021).
89. Kivelson, S. & Kivelson, S. Understanding complexity. *Nat. Phys.* **14**, 426–427 (2018).
90. Wang, Q. et al. Predicting the propensity for thermally activated β events in metallic glasses via interpretable machine learning. *npj Comput. Mater.* **6**, 194 (2020).
91. Miao, S., Liu, M. & Li, P. Interpretable and generalizable graph learning via stochastic attention mechanism. In *Proc. 39th International Conference on Machine Learning, Volume 162 of Proceedings of Machine Learning Research* (eds Chaudhuri, K. et al.) 15524–15543 (PMLR, 2022).
92. Duede, E. Deep learning opacity in scientific discovery. *Philos. Sci.* **90**, 1089–1099 (2023).
93. Glielmo, A., Zeni, C., Cheng, B., Csányi, G. & Laio, A. Ranking the information content of distance measures. *PNAS Nexus* **1**, pgac039 (2022).
94. Sandberg, J., Voigtmann, T., Devijver, E. & Jakse, N. Feature selection for high-dimensional neural network potentials with the adaptive group lasso. *Mach. Learn. Sci. Technol.* **5**, 025043 (2024).
95. Sharma, A., Liu, C. & Ozawa, M. Selecting relevant structural features for glassy dynamics by information imbalance. *J. Chem. Phys.* **161**, 184506 (2024).
96. Berthier, L., Flenner, E. & Szamel, G. Glassy dynamics in dense systems of active particles. *J. Chem. Phys.* **150**, 200901 (2019).
97. Janzen, G. & Janssen, L. M. C. Rejuvenation and memory effects in active glasses induced by thermal and active cycling. *Phys. Rev. Res.* **6**, 023257 (2024).
98. Janzen, G. et al. Dead or alive: distinguishing active from passive particles using supervised learning. *Europhys. Lett.* **143**, 17004 (2023).
99. Janzen, G. et al. Classifying the age of a glass based on structural properties: a machine learning approach. *Phys. Rev. Mater.* **8**, 025602 (2024).
100. Scalliet, C., Guiselin, B. & Berthier, L. Excess wings and asymmetric relaxation spectra in a facilitated trap model. *J. Chem. Phys.* **155**, 064505 (2021).
101. Guiselin, B., Scalliet, C. & Berthier, L. Microscopic origin of excess wings in relaxation spectra of supercooled liquids. *Nat. Phys.* **18**, 468–472 (2022).
102. Nicolas, A., Ferrero, E. E., Martens, K. & Barrat, J.-L. Deformation and flow of amorphous solids: Insights from elastoplastic models. *Rev. Mod. Phys.* **90**, 045006 (2018).
103. Ozawa, M. & Biroli, G. Elasticity, facilitation and dynamic heterogeneity in glass-forming liquids. *Phys. Rev. Lett.* **130**, 138201 (2023).
104. Tahaei, A., Biroli, G., Ozawa, M., Popović, M. & Wyart, M. Scaling description of dynamical heterogeneity and avalanches of relaxation in glass-forming liquids. *Phys. Rev. X* **13**, 031034 (2023).
105. Lerbinger, M., Barbot, A., Vandembroucq, D. & Patinet, S. Relevance of shear transformations in the relaxation of supercooled liquids. *Phys. Rev. Lett.* **129**, 195501 (2022).
106. Chacko, R. N. et al. Elastoplasticity mediates dynamical heterogeneity below the mode coupling temperature. *Phys. Rev. Lett.* **127**, 048002 (2021).
107. Monthus, C. & Bouchaud, J. P. Models of traps and glass phenomenology. *J. Phys. A Math. Gen.* **29**, 3847 (1996).
108. Ridout, S. A., Tah, I. & Liu, A. J. Building a “trap model” of glassy dynamics from a local structural predictor of rearrangements. *Europhys. Lett.* **144**, 47001 (2023).
109. Ridout, S. A. & Liu, A. J. The dynamics of machine-learned “softness” in supercooled liquids describe dynamical heterogeneity. Preprint at <https://doi.org/10.48550/arXiv.2406.05868> (2024).
110. Ciarella, S. et al. Finding defects in glasses through machine learning. *Nat. Commun.* **14**, 4229 (2023).
111. Richard, D., Kapteijns, G. & Lerner, E. Detecting low-energy quasilocalized excitations in computer glasses. *Phys. Rev. E* **108**, 044124 (2023).
112. Scalliet, C., Guiselin, B. & Berthier, L. Thirty milliseconds in the life of a supercooled liquid. *Phys. Rev. X* **12**, 041028 (2022).
113. Ediger, M. D. Spatially heterogeneous dynamics in supercooled liquids. *Annu. Rev. Phys. Chem.* **51**, 99–128 (2000).
114. Tong, H. & Tanaka, H. Structural order as a genuine control parameter of dynamics in simple glass formers. *Nat. Commun.* **10**, 5596 (2019).
115. Lačević, N., Starr, F. W., Schröder, T. B. & Glotzer, S. C. Spatially heterogeneous dynamics investigated via a time-dependent four-point density correlation function. *J. Chem. Phys.* **119**, 7372–7387 (2003).
116. Flenner, E., Zhang, M. & Szamel, G. Analysis of a growing dynamic length scale in a glass-forming binary hard-sphere mixture. *Phys. Rev. E* **83**, 051501 (2011).
117. Jiang, X., Tian, Z., Li, K. & Hu, W. A geometry-enhanced graph neural network for learning the smoothness of glassy dynamics from static structure. *J. Chem. Phys.* **159**, 144504 (2023).
118. Swendsen, R. H. & Wang, J.-S. Replica Monte Carlo simulation of spin-glasses. *Phys. Rev. Lett.* **57**, 2607 (1986).
119. Berthier, L., Coslovich, D., Ninarello, A. & Ozawa, M. Equilibrium sampling of hard spheres up to the jamming density and beyond. *Phys. Rev. Lett.* **116**, 238002 (2016).
120. Fan, Z. & Ma, E. Predicting orientation-dependent plastic susceptibility from static structure in amorphous solids via deep learning. *Nat. Commun.* **12**, 1506 (2021).
121. Du, T. et al. Predicting fracture propensity in amorphous alumina from its static structure using machine learning. *ACS Nano* **15**, 17705–17716 (2021).
122. Font-Clos, F. et al. Predicting the failure of two-dimensional silica glasses. *Nat. Commun.* **13**, 2820 (2022).
123. Liu, H., Fu, Z., Yang, K., Xu, X. & Bauchy, M. Machine learning for glass science and engineering: a review. *J. Non Cryst. Solids* **557**, 119419 (2021).
124. Cassar, D. R. GlassNet: a multitask deep neural network for predicting many glass properties. *Ceram. Int.* **49**, 36013–36024 (2023).
125. Tandia, A., Onbasli, M. C. & Mauro, J. C. in *Springer Handbook of Glass* 1157–1192 (2019).
126. Merchant, A. et al. Scaling deep learning for materials discovery. *Nature* **624**, 80–85 (2023).
127. Unke, O. T. et al. Machine learning force fields. *Chem. Rev.* **121**, 10142–10186 (2021).
128. Volpe, G. et al. Roadmap on deep learning for microscopy. Preprint at <https://doi.org/10.48550/arXiv.2303.03793> (2023).
129. Midtvedt, B., Pineda, J., Klein Morberg, H., Manzo, C. & Volpe, G. DeepTrack2. <https://github.com/softmatterlab/DeepTrack2> (2024).
130. Gabrié, M. Mean-field inference methods for neural networks. *J. Phys. A Math. Theor.* **53**, 223002 (2020).
131. Merchant, A., Metz, L., Schoenholz, S. S. & Cubuk, E. D. Learn2hop: learned optimization on rough landscapes. In *International Conference on Machine Learning* 7643–7653 (PMLR, 2021).
132. Gabrié, M., Ganguli, S., Lucibello, C. & Zecchina, R. Neural networks: from the perceptron to deep nets. Preprint at <https://doi.org/10.48550/arXiv.2304.06636> (2023).
133. Bonnaire, T. et al. High-dimensional non-convex landscapes and gradient descent dynamics. *J. Stat. Mech.* **104004** (2024).
134. Mézard, M. Spin glass theory and its new challenge: structured disorder. *Indian J. Phys.* **98**, 3757 (2023).
135. Vaswani, A. Attention is all you need. In *31st Conference on Neural Information Processing Systems* (NIPS, 2017).
136. Jumper, J. et al. Highly accurate protein structure prediction with AlphaFold. *Nature* **596**, 583–589 (2021).
137. Baek, M. et al. Accurate prediction of protein structures and interactions using a three-track neural network. *Science* **373**, 871–876 (2021).
138. Bratholm, L. A. et al. A community-powered search of machine learning strategy space to find NMR property prediction models. *PLoS ONE* **16**, e0253612 (2021).
139. Qin, Y. et al. A dual-stage attention-based recurrent neural network for time series prediction. Preprint at <https://doi.org/10.48550/arXiv.1704.02971> (2017).
140. Chapelle, O., Schölkopf, B. & Zien, A. (eds.) *Semi-Supervised Learning* (MIT Press, 2006).
141. Rong, Y. et al. Self-supervised graph transformer on large-scale molecular data. *Adv. Neural Inf. Process. Syst.* **33**, 12559–12571 (2020).
142. Magar, R., Wang, Y. & Barati Farimani, A. Crystal twins: self-supervised learning for crystalline material property prediction. *npj Comput. Mater.* **8**, 231 (2022).
143. Zhang, Z. et al. Graph self-supervised learning for optoelectronic properties of organic semiconductors. In *ICML 2022 2nd AI for Science Workshop* (2022).
144. Kaelbling, L. P., Littman, M. L. & Moore, A. W. Reinforcement learning: a survey. *J. Artif. Intell. Res.* **4**, 237–285 (1996).
145. Shin, K. et al. Enhancing biomolecular sampling with reinforcement learning: a tree search molecular dynamics simulation method. *ACS Omega* **4**, 138530–13862 (2019).
146. Fan, C. et al. Searching for spin glass ground states through deep reinforcement learning. *Nat. Commun.* **14**, 725 (2023).
147. Ahuja, K., Green, W. H. & Li, Y.-P. Learning to optimize molecular geometries using reinforcement learning. *J. Chem. Theory Comput.* **17**, 818–825 (2021).
148. Bihani, V., Manchanda, S., Sastry, S., Ranu, S. & Krishnan, N. A. Stridernet: a graph reinforcement learning approach to optimize atomic structures on rough energy landscapes. In *International Conference on Machine Learning* 2431–2451 (PMLR, 2023).
149. Bojesen, T. A. Policy-guided Monte Carlo: reinforcement-learning Markov chain dynamics. *Phys. Rev. E* **98**, 063303 (2018).
150. Galliano, L., Rende, R. & Coslovich, D. Policy-guided Monte Carlo on general state spaces: application to glass-forming mixtures. *J. Chem. Phys.* **161**, 064503 (2024).
151. Christiansen, H., Errica, F. & Alesiani, F. Self-tuning Hamiltonian Monte Carlo for accelerated sampling. *J. Chem. Phys.* **159**, 234109 (2023).
152. Gabrié, M., Rotskoff, G. M. & Vanden-Eijnden, E. Adaptive Monte Carlo augmented with normalizing flows. *Proc. Natl Acad. Sci. USA* **119**, e2109420119 (2022).
153. Ninarello, A., Berthier, L. & Coslovich, D. Models and algorithms for the next generation of glass transition studies. *Phys. Rev. X* **7**, 021039 (2017).
154. Berthier, L. & Reichman, D. R. Modern computational studies of the glass transition. *Nat. Rev. Phys.* **5**, 102–116 (2023).
155. Noé, F., Olsson, S., Köhler, J. & Wu, H. Boltzmann generators: sampling equilibrium states of many-body systems with deep learning. *Science* **365**, eaaw1147 (2019).
156. Wu, D., Wang, L. & Zhang, P. Solving statistical mechanics using variational autoregressive networks. *Phys. Rev. Lett.* **122**, 080602 (2019).
157. Köhler, J., Klein, L. & Noé, F. Equivariant flows: exact likelihood generative learning for symmetric densities. In *International Conference on Machine Learning* 5361–5370 (PMLR, 2020).
158. Dibak, M., Klein, L., Krämer, A. & Noé, F. Temperature steerable flows and Boltzmann generators. *Phys. Rev. Res.* **4**, L042005 (2022).
159. Invernizzi, M., Krämer, A., Clementi, C. & Noé, F. Skipping the replica exchange ladder with normalizing flows. *J. Phys. Chem. Lett.* **13**, 11643–11649 (2022).

160. Xu, M. et al. Geodiff: a geometric diffusion model for molecular conformation generation. Preprint at <https://doi.org/10.48550/arXiv.2203.02923> (2022).
161. Coretti, A., Falkner, S., Geissler, P. & Dellago, C. Learning mappings between equilibrium states of liquid systems using normalizing flows. Preprint at <https://doi.org/10.48550/arXiv.2208.10420> (2022).
162. van Leeuwen, S., de Alba Ortíz, A. P. & Dijkstra, M. A Boltzmann generator for the isobaric-isothermal ensemble. Preprint at <https://doi.org/10.48550/arXiv.2305.08483> (2023).
163. Jung, G., Biroli, G. & Berthier, L. Normalizing flows as an enhanced sampling method for atomistic supercooled liquids. *Mach. Learn. Sci. Technol.* **5**, 035053 (2024).
164. McNaughton, B., Milošević, M., Perali, A. & Pilati, S. Boosting Monte Carlo simulations of spin glasses using autoregressive neural networks. *Phys. Rev. E* **101**, 053312 (2020).
165. Hibat-Allah, M., Inack, E. M., Wiersema, R., Melko, R. G. & Carrasquilla, J. Variational neural annealing. *Nat. Mach. Intell.* **3**, 952–961 (2021).
166. Wu, D., Rossi, R. & Carleo, G. Unbiased Monte Carlo cluster updates with autoregressive neural networks. *Phys. Rev. Res.* **3**, L042024 (2021).
167. Inack, E. M., Morawetz, S. & Melko, R. G. Neural annealing and visualization of autoregressive neural networks in the Newman–Moore model. *Condens. Matter* **7**, 38 (2022).
168. Ciarella, S., Trinquier, J., Weigt, M. & Zamponi, F. Machine-learning-assisted Monte Carlo fails at sampling computationally hard problems. *Mach. Learn. Sci. Technol.* **4**, 010501 (2023).
169. Schuetz, M. J., Brubaker, J. K., Zhu, Z. & Katzgraber, H. G. Graph coloring with physics-inspired graph neural networks. *Phys. Rev. Res.* **4**, 043131 (2022).
170. Schuetz, M. J., Brubaker, J. K. & Katzgraber, H. G. Combinatorial optimization with physics-inspired graph neural networks. *Nat. Mach. Intell.* **4**, 367–377 (2022).
171. Albergo, M. S., Kanwar, G. & Shanahan, P. E. Flow-based generative models for Markov chain Monte Carlo in lattice field theory. *Phys. Rev. D* **100**, 034515 (2019).
172. Kanwar, G. et al. Equivariant flow-based sampling for lattice gauge theory. *Phys. Rev. Lett.* **125**, 121601 (2020).
173. de Haan, P., Rainone, C., Cheng, M. C. & Bondesan, R. Scaling up machine learning for quantum field theory with equivariant continuous flows. Preprint at <https://doi.org/10.48550/arXiv.2110.02673> (2021).
174. Gerdes, M., de Haan, P., Rainone, C., Bondesan, R. & Cheng, M. C. Learning lattice quantum field theories with equivariant continuous flows. *SciPost Phys.* **15**, 238 (2023).
175. Luo, D., Carleo, G., Clark, B. K. & Stokes, J. Gauge equivariant neural networks for quantum lattice gauge theories. *Phys. Rev. Lett.* **127**, 276402 (2021).
176. Marchand, T., Ozawa, M., Biroli, G. & Mallat, S. Wavelet conditional renormalization group. Preprint at <https://doi.org/10.48550/arXiv.2207.04941> (2022).
177. Angelini, M. C. & Ricci-Tersenghi, F. Modern graph neural networks do worse than classical greedy algorithms in solving combinatorial optimization problems like maximum independent set. *Nat. Mach. Intell.* **5**, 29–31 (2023).
178. Boettcher, S. Inability of a graph neural network heuristic to outperform greedy algorithms in solving combinatorial optimization problems. *Nat. Mach. Intell.* **5**, 24–25 (2023).
179. Boettcher, S. Deep reinforced learning heuristic tested on spin-glass ground states: the larger picture. *Nat. Commun.* **14**, 5658 (2023).
180. Ghio, D., Dandi, Y., Krzakala, F. & Zdeborová, L. Sampling with flows, diffusion and autoregressive neural networks: a spin-glass perspective. *Proc. Natl Acad. Sci. USA* **121**, e2311810121 (2024).

Acknowledgements

This paper originates from discussions and interactions at the AISSAI (AI for science, science for AI) workshop on ‘Machine Learning Glasses’ held in November 2022 in Paris. This workshop was organized by G.B., L.B. and G.J. The authors thank all participants for their attendance, discussions and feedback, in particular A. Banerjee, L. Janssen, M. Ruiz Garcia, S. Patinet, C. Scalliet, D. Richard, J. Rottler, O. Dauchot and O. Kukhareno for their valuable contributions. F.S.P. is supported by a public grant overseen by the French National Research Agency (ANR) through the programme UDOPIA, project funded by the ANR-20-THIA-0013-01. F.S.P. was granted access to the HPC resources of IDRIS under the allocation 2022-AD011014066 made by GENCI. H.S. acknowledges computational resources provided by ‘Joint Usage/Research Center for Interdisciplinary Large-scale Information Infrastructures (JHPCN)’ and ‘High Performance Computing Infrastructure (HPCI)’ in Japan (project ID: jh230064). A.J.L. is supported by the Simons Foundation via the Investigator Award #327939. In addition, A.J.L. thanks CCB at the Flatiron Institute and the Isaac Newton Institute for Mathematical Sciences under the programme ‘New Statistical Physics in Living Matter’ (EPSRC grant EP/R014601/1) for the support and hospitality. This work was supported by a grant from the Simons Foundation (#454933 to L.B., #454935 to G.B.). G.B. acknowledges funding from the French government under the management of Agence Nationale de la Recherche as part of the ‘Investissements d’avenir’ programme, reference ANR-19-P3IA-0001 (PRAIRIE 3IA Institute).

Author contributions

G.J., L.B. and G.B. coordinated the manuscript and submission. D.C., L.F., A.J.L. and G.J. drafted original versions of the sections from ‘Machine learning locally favoured structures’ to ‘Performance metrics and benchmarking’. V.B., G.V., F.Z. and F.P.L. drafted original versions of the ‘Outlook’ section. L.F., R.M.A., F.P.L., F.S.P., D.C., H.S. and G.J. devised the benchmarks. All authors participated in proofreading and corrections.

Competing interests

The authors declare no competing interests.

Additional information

Supplementary information The online version contains supplementary material available at <https://doi.org/10.1038/s42254-024-00791-4>.

Peer review information *Nature Reviews Physics* thanks Han Liu and the other, anonymous, referee(s) for their contribution to the peer review of this work.

Publisher’s note Springer Nature remains neutral with regard to jurisdictional claims in published maps and institutional affiliations.

Springer Nature or its licensor (e.g. a society or other partner) holds exclusive rights to this article under a publishing agreement with the author(s) or other rightsholder(s); author self-archiving of the accepted manuscript version of this article is solely governed by the terms of such publishing agreement and applicable law.

© Springer Nature Limited 2025